

Ultraviolet coherent random lasing in randomly assembled SnO₂ nanowires

H. Y. Yang,¹ S. F. Yu,^{1,a)} S. P. Lau,² S. H. Tsang,¹ G. Z. Xing,³ and T. Wu³

¹*School of Electrical and Electronic Engineering, Nanyang Technological University, Singapore 639798, Singapore*

²*Department of Applied Physics, The Hong Kong Polytechnic University, Hung Hum, Kowloon, Hong Kong*

³*School of Physical and Mathematical Sciences, Nanyang Technological University, Singapore 639798, Singapore*

(Received 14 May 2009; accepted 2 June 2009; published online 19 June 2009)

Although nanostructured SnO₂ exhibited ultraviolet stimulated emission at room temperature, the low emission intensities and occurrence of gain saturation restricted them to be considered as luminescent materials for semiconductor lasers. In this letter, we find that a large ultraviolet excitonic gain can be obtained from SnO₂ nanowires coated with an amorphous layer. Under effective pumping, ultraviolet coherent random lasing can be realized from randomly assembled SnO₂ nanowires at room temperature. © 2009 American Institute of Physics.

[DOI: 10.1063/1.3157842]

Nanostructured SnO₂ materials, which have a wide bandgap and high exciton-binding energy, are considered to be a promising optical-grade material for the realization of passive optoelectronic devices. Various structural and morphological forms of nanostructured SnO₂ materials such as nanowires, nanoribbons, nanotubes, and nanobelts have been fabricated over the past several years to realize high performance dye-based solar cells, photoconductor, optical waveguide, and optical sensors.^{1,2} However, it is seldom observed direct band-to-band radiative recombination from the SnO₂ nanostructures due to its large amount of defect states inside the bandgap. Most of the ultraviolet to visible emission bands, which used to have low intensity at room temperature, are related to the defect and impurity-related photoluminescence (PL).^{3,4} Recently, room-temperature ultraviolet stimulated emission, which is attributed to the localization of excitons at the shallow trapped states, is observed from SnO₂ nanowires under optical excitation.⁵ However, the intensity of excitonic stimulated emission is shown to be weak and saturated at low excitation intensities. Therefore, under normal circumstance, SnO₂ materials cannot be considered as suitable luminescent materials for semiconductor lasers. In this letter, we demonstrated a large excitonic gain can be obtained from SnO₂ nanowires coated with an amorphous layer (i.e., a layer of surface defects) via effective optical excitation to sustain ultraviolet coherent random lasing at room temperature.

The randomly assembled SnO₂ nanowires were fabricated by using a vapor transport method and the growth was taken place in a horizontal tube furnace (Lindberg/Blue Mini-Mite). To prepare the source powder for the growth process, a mixture of SnO₂ and graphite (weight ratio 1:1) was ground in an agate mortar for half an hour. A clean Si wafer of size 6×8 mm², which was coated with a 2 nm thick Au film, was used as the growth substrate. Au was used as catalyst to assist the SnO₂ nanowires synthesis upon carbothermal evaporation of SnO₂ powders. The substrate was placed at the center of a quartz tube. The quartz tube was then inserted into the horizontal tube furnace with the source

located at the furnace center. Ar mixed with 5% of O₂ was used as the carry gas and the pressure inside the quartz tube was maintained at 20 mbar. During the growth, temperature of the furnace was ramped up to 1100 °C with a rate of 20 °C/min and the substrate temperature was calibrated to about 800 °C. After the growth of 1 h, a ~2 μm thick of white-blue film was formed on the Si substrate.

Figure 1(a) plots the x-ray diffraction (XRD) pattern of as-grown SnO₂ nanowires. All the diffraction peaks can be indexed to the tetragonal rutile SnO₂. The energy dispersive x-ray spectroscopy spectrum of the sample, in which only peaks with Sn and O elements are observed, is also shown in Fig. 1(b). Figures 1(c)–1(e) are the SEM images of the SnO₂ nanowires. It is observed that the nanowires are closely packed together to form randomly assembled nanowires. Furthermore, the nanowires, which have preferred orientation of (100) direction, have average length and width of ~10 μm and ~100 nm, respectively. Figure 1(f) shows a high-resolution transmission electron microscopy (HRTEM) image of the nanowire. It is observed that the nanowire has good crystallinity of tetragonal rutile SnO₂ structure with lattice constants of *a* and *c* equal to 4.72 and 3.17 Å, respectively. It is also noted that the surface of the nanowires is

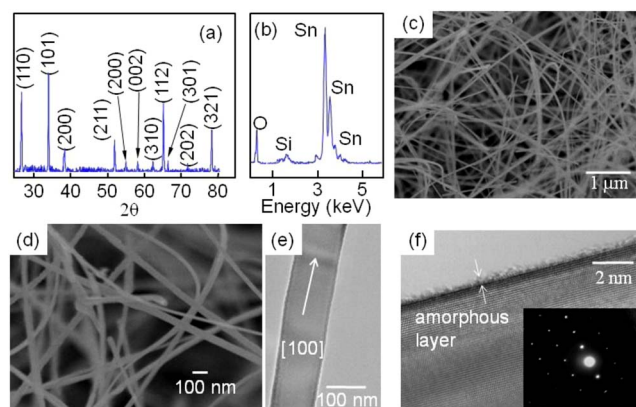


FIG. 1. (Color online) (a) XRD pattern, (b) EDS spectrum, (c) low-magnification SEM image, and [(d) and (e)] high-magnification SEM image of the randomly assembled SnO₂ nanowires. (f) HRTEM of a SnO₂ nanowire and the insert shows the corresponding SAED pattern.

^{a)}Author to whom correspondence should be addressed. Electronic mail: esfyu@ntu.edu.sg.

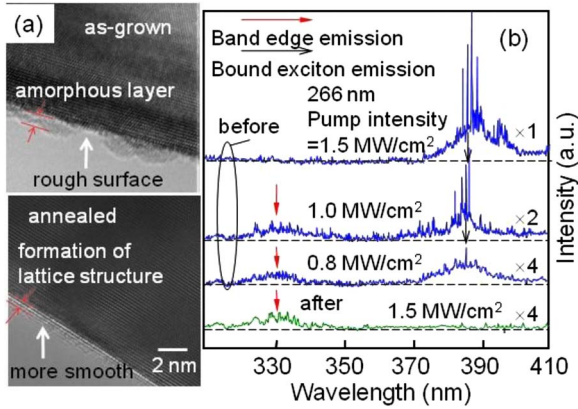


FIG. 2. (Color online) (a) HRTEM of a SnO_2 nanowire before and after thermal annealing. (b) PL spectra of the randomly assembled SnO_2 nanowires before and after thermal annealing under 266 nm optical pumping.

coated with an amorphous layer of an average thickness of 1.5 nm. This amorphous layer can be attributed to the formation of shallow trapped states for the occupation of excitons.⁵

During the formation of SnO_2 nanowires, it is no surprised that the nanowires can be coated with an amorphous layer (in which Sn interstitials, oxygen vacancies, and other intrinsic defects can be formed⁶) due to incomplete oxidation. This is because the oxidation reaction of SnO to SnO_2 nanowires⁷ is started to respond at 780 °C (Ref. 8) so that the complete oxidation at the nanowires' surface may require substrate temperature higher than 800 °C. Figure 2(a) compares the HRTEM image of the SnO_2 nanowires before and after thermal annealing at 900 °C in O_2 for 10 min. It is observed that the amorphous layer is replaced by the formation of few crystalline layers. Figure 2(b) compares the PL of the SnO_2 nanowires before and after annealing. During the measurement, the samples were optically excited by a frequency-quadruplet 266 nm pulsed neodymium doped yttrium aluminum garnet (Nd:YAG) laser with 120 ps pulse width and 10 Hz repetition rate. A spherical lens was used to focus a pump beam of ~ 1 mm in diameter onto the samples' surface. Emission was collected in the direction perpendicular to the surface of the samples. It is observed that, although both samples exhibit a weak bandedge emission at around 340 nm, only the as-grown SnO_2 nanowires have emission (i.e., sharp peaks with linewidth < 0.4 nm occurs at excitation power greater than 0.8 MW/cm^2) at around 387 nm. However, visible band, which presence is mainly due to oxygen vacancies, was not observed from the emission spectra before and after annealing. The above experiment has verified that strong excitonic radiative recombination is due to the presence of large surface-defect area (i.e., large amount of shallow trapped states of bound excitons) in the SnO_2 nanowires.

It has been shown that the bandgap of the SnO_2 can be reduced to ~ 3.38 eV due to exciton-phonon coupling at room temperature.⁹ If excitation source with wavelength of 266 nm (i.e., 4.66 eV) is used, the corresponding excitation energy will cause nonradiative recombination at the continuum states above the conduction band. As a result, the efficiency to generate weakly bound excitons at the shallow trapped states induced by the presence of the amorphous layer will be reduced. Hence, a frequency-tripled 355 nm (3.49 eV) pulsed Nd:YAG laser with 120 ps pulse width and

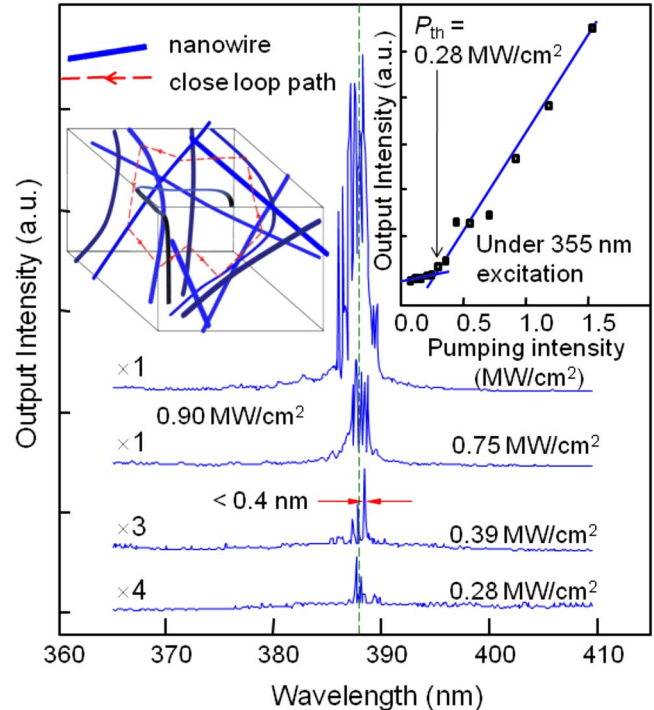


FIG. 3. (Color online) Emission spectra of the randomly assembled SnO_2 nanowires under the excitation of 355 nm optical pumping. The corresponding light-light curve is also shown in the figure. The insert schematic shows the formation of close loop path of light inside the randomly assembled SnO_2 nanowires.

10 Hz repetition rate was used as the excitation source to repeat the above measurement. It is believed that the 355 nm excitation energy is sufficient to excite carriers to the conduction band edge of SnO_2 before relaxed to the shallow trapped states and avoided nonradiative absorption at the continuum states. Figure 3 shows the emission spectra and light-light curve of the randomly assembled nanowires. It is observed that when excitation power exceeds a threshold of ~ 0.28 MW/cm^2 , sharp peaks (i.e., lasing modes) at around 387 nm with linewidth less than 0.4 nm emerged from the emission spectra. In addition, the intensities of sharp peaks are much higher than the intensity of background noise level [the contrast is much higher than that given in Fig. 2(b)]. As the pumping threshold is reduced from 0.8 to 0.28 MW/cm^2 by using 355 nm pumping, the corresponding conversion efficiency has also been increased by 2.9 times. It is also observed that the wavelength of lasing peaks is independent on the pump intensity. This is consistent with the fact that it is of an excitonic origin and excitonic Mott transition has not been reached.

From the SEM image given in Fig. 1(c), it is noted that, although the nanowires are closely packed, air is filled between the nanowires. As the refractive index of SnO_2 nanowires is about 2.0 at 387 nm, large contrast in refractive index between SnO_2 and air may provide a strong scattering. The scattering mean free path l of the randomly assembled SnO_2 nanowires can be estimated by the coherent back-scattering experiment using a 405 nm ps diode laser as the probe light. It is estimated that l is about 0.8 times the diode laser wavelength. Hence, as l is less than the operating wavelength, light may be returned to a scatter from which it was scattered before and thereby forming closed loop paths. This shows that the scattering strength of the randomly assembled

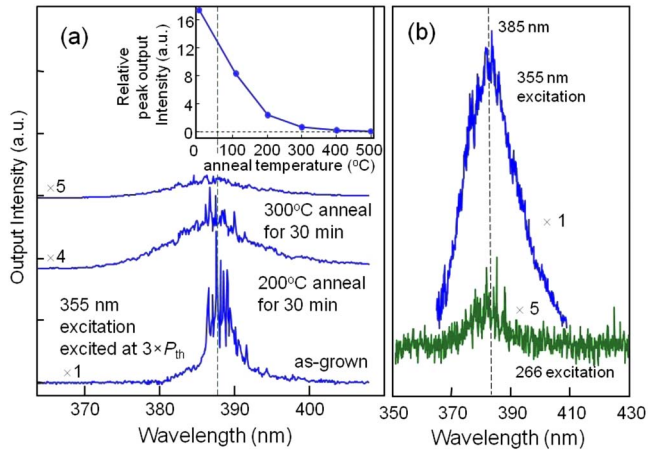


FIG. 4. (Color online) (a) Emission spectra of the randomly assembled SnO_2 nanowires before and after thermal annealing at 100–500 °C for 30 min. The inset shows the variation in peak emission intensity vs the annealing temperature. (b) Emission spectra of the annealed (at 500 °C for 30 min) SnO_2 nanowires after the exposure to Sn vapor at 400 °C for 5 min.

nanowires is sufficient to achieve coherent feedback. Hence, it is believed that the sharp peak represents a closed loop path of light (i.e., see the inset of Fig. 3), which randomly formed a cavity mode inside the random cavity, due to the coherent optical feedback of scattering light. However, if the density and size of the SnO_2 nanowires are varied significantly from the current values, closed loop paths may not be formed. In fact, it can be shown that (i) the emission spectra are different at different observation angles and (ii) $A_{\text{th}}^{-2/3}$ versus P_{th}^{-1} exhibits a linear relationship where A_{th} is threshold excitation area and P_{th} threshold pump intensity. Hence, all of the essential characteristics of random laser action have been observed, the lasing mechanism of the sample is verified to be random laser action.

O vacancies (V_{O}) and Sn interstitials (Sn_i), which are believed to act as shallow donor levels lying below the conduction band, induce high n -type conductivity of nonstoichiometric SnO_2 .⁶ However, it has been shown that V_{O} contributed to the room-temperature efficient PL emission at visible spectrum.⁵ Therefore, Sn_i may be the dominant surface defect leads to the generation of ultraviolet emission. It is estimated that Sn_i has lower formation energy than that of V_{O} so that thermal annealing of the SnO_2 nanowires at low temperature may cause the out diffusion of Sn_i as well as the reduction in ultraviolet emission.⁶ Figure 4(a) shows the emission spectra of the randomly assembled SnO_2 nanowires after thermal annealing at 100–500 °C for 30 min in O_2 . The inset of Fig. 4(a) plots the variation in relative peak intensities versus different annealing temperature. It is observed that the ultraviolet emission can be significantly reduced even the annealing temperature is as low as 300 °C.

The HRTEM image of the sample under thermal annealing at 500 °C (not shown) has shown similar surface profile to that given in Fig. 2(a) (annealed).

In order to verify that the ultraviolet emission is due to Sn_i , the annealed sample at 500 °C was exposed to Sn vapor inside the quartz tube by heating Sn powder to 400 °C. This annealing temperature was chosen to achieve a relatively high Sn vapor pressure for the reaction. In addition, the quartz tube was maintained at 20 mbar with a flow of Ar gas to avoid the formation of V_{O} . Hence, the Sn vapor will diffuse into Sn– O_2 site to form (i.e., Sn_i) as the temperature is not high enough to form bonding. Figure 4(b) shows the emission spectra of the SnO_2 nanowires exposed in Sn vapor for 5 min. Emission peak at around 384 nm is observed indicated that Sn_i is strongly related to the defect emission at ultraviolet wavelength. As the 355 nm excitation wavelength is more effective than that of 266 nm, the corresponding defect radiative recombination mechanism should be similar to that of the as-grown SnO_2 nanowires. However, the magnitude of emission peak is significantly reduced by about 10 times. This is because Sn vapor can only reach few top layers of the SnO_2 nanowires to form Sn_i . We noted that the prolong exposure to Sn vapor do not enhance the emission intensities as Sn layer may form on the surface of SnO_2 nanowires. Therefore, it is verified that Sn_i is the main cause of ultraviolet excitonic gain in SnO_2 nanowires.

In conclusion, we have shown that it is possible to manipulate the surface-state of SnO_2 nanowires such that the density of bound excitons can be significantly increased. With effective pumping of the bound excitons to the shallow trapped state, a large quantity of density of state for the bound excitons can be obtained. This will lead to a large excitonic gain at ultraviolet regime to support coherent random laser action inside the randomly assembled SnO_2 nanowires.

The work was supported by LKYPDF 2/08 startup grant.

- ¹Z. R. Dai, Z. W. Pan, and Z. L. Wang, *Adv. Funct. Mater.* **13**, 9 (2003).
- ²G. Z. Shen, P. C. Chen, K. M. Ryu, and C. W. Zhou, *J. Mater. Chem.* **19**, 828 (2009).
- ³M. Fang, X. Tan, B. C. Cheng, and L. Zhang, *J. Mater. Chem.* **19**, 1320 (2009).
- ⁴S. Lettieri, M. Causa, A. Setaro, F. Trani, V. Barone, D. Ninno, and P. Maddalena, *J. Chem. Phys.* **129**, 244710 (2008).
- ⁵W. C. Zhou, R. B. Liu, Q. Wan, Q. L. Zhang, A. L. Pan, L. Guo, and B. S. Zou, *J. Phys. Chem. C* **113**, 1719 (2009).
- ⁶C. Kilic and A. Zunger, *Phys. Rev. Lett.* **88**, 095501 (2002).
- ⁷C. L. Zheng, J. G. Wan, Y. Cheng, D. H. Cu, and Y. J. Zhan, *Int. J. Mod. Phys. B* **19**, 2811 (2005).
- ⁸Y. K. Liu, C. L. Zheng, W. Z. Wang, Y. J. Zhan, and G. H. Wang, *J. Cryst. Growth* **233**, 8 (2001).
- ⁹R. B. Liu, Y. J. Chen, F. F. Wang, L. Cao, A. L. Pan, G. Z. Yang, T. H. Wang, and B. S. Zou, *Physica E (Amsterdam)* **39**, 223 (2007).